Annals of Biomedical Engineering, Vol. 45, No. 6, June 2017 (© 2017) pp. 1387–1398
DOI: 10.1007/s10439-017-1822-8

Stiffness of Protease Sensitive and Cell Adhesive PEG Hydrogels Promotes Neovascularization *In Vivo*

RYAN M. SCHWELLER,[1] ZI JUN WU,[2] BRUCE KLITZMAN,[1,2] and JENNIFER L. WEST[1]

[1]Department of Biomedical Engineering, Duke University, Durham, NC 27708, USA; and [2]Kenan Plastic Surgery Research Labs, Duke University School of Medicine, Durham, NC 27710, USA

(*Received 19 January 2017; accepted 15 March 2017; published online 30 March 2017*)

Associate Editor Konstantinos Konstantopoulos oversaw the review of this article.

Abstract—Materials that support the assembly of new vasculature are critical for regenerative medicine. Controlling the scaffold's mechanical properties may help to optimize neovascularization within implanted biomaterials. However, reducing the stiffness of synthetic hydrogels usually requires decreasing polymer densities or increasing chain lengths, both of which accelerate degradation. We synthesized enzymatically-degradable poly(ethylene glycol) hydrogels with compressive moduli from 2 to 18 kPa at constant polymer density, chain length, and proteolytic degradability by inserting an allyloxycarbonyl functionality into the polymer backbone. This group competes with acrylates during photopolymerization to alter the crosslink network structure and reduce the hydrogel's stiffness. Hydrogels that incorporated (soft) or lacked (stiff) this group were implanted subcutaneously in rats to investigate the role of stiffness on host tissue interactions. Changes in tissue integration were quantified after 4 weeks *via* the hydrogel area replaced by native tissue (tissue area fraction), yielding 0.136 for softer vs. 0.062 for stiffer hydrogels. Including soluble FGF-2 and PDGF-BB improved these responses to 0.164 and 0.089, respectively. Softer gels exhibited greater vascularization with 8.6 microvessels mm^{-2} compared to stiffer gels at 2.4 microvessels mm^{-2}. Growth factors improved this to 11.2 and 4.9 microvessels mm^{-2}, respectively. Softer hydrogels tended to display more sustained responses, promoting neovascularization and tissue integration in synthetic scaffolds.

Keywords—Angiogenesis, Endothelial cell, Inflammation, Mechanical properties.

INTRODUCTION

Vascularization is necessary for cell survival and function in almost all tissues, providing delivery of oxygen and nutrients as well as the removal of waste products. Therefore, the incorporation of microvascular networks into engineered tissue constructs that can form anastamoses with host vasculature is critical to facilitate mass transport and promote tissue regeneration. The creation of these vascularized materials has largely focused on recapitulating key cell-extracellular matrix (ECM) interactions and the mechanical properties of native vascularized tissues in engineered biomaterials with the rationale that accurate reproduction of the native tissue environment will improve neovascularization for various applications.[2] To create these complex environments, a wide variety of synthetic and naturally-derived materials have been developed which are able to induce the formation of vessel-like networks through the recruitment of endogenous vasculature that integrates with the material or the direct encapsulation and delivery of endothelial and mural support cell sources which can then assemble into new vascular networks.[25,29,32] However, understanding the influence of various ECM components and material mechanics on cellular behaviors remains paramount for the design and optimization of new biomaterials capable of promoting neovascularization.

To dissect the individual effects of biochemical and mechanical components on vascularization responses, increasing interest has been placed on hydrogel-forming materials that are synthetic and biologically inert, allowing them to be custom tailored with various ECM-derived cues. In particular, poly(ethylene glycol) diacrylate (PEGDA)–based hydrogels have shown great promise towards these applications as they resist non-specific protein adsorption and encode no innate biological activity.[19] This allows the fabrication of three dimensional (3D) PEGDA hydrogels by photopolymerization as well as customization through the

Address correspondence to Jennifer L. West, Department of Biomedical Engineering, Duke University, Durham, NC 27708, USA. Electronic mail: jennifer.l.west@duke.edu

incorporation of various acrylate-functionalized peptides, proteins, and growth factors.[23,26] In addition, these hydrogels can be rendered cell degradable by incorporating protease-sensitive peptides into the polymer backbones that encode sites for matrix metalloproteinase (MMP), plasmin, or cathepsin -based cleavage.[17,39] Together, these capabilities have allowed these photopolymerizable PEGDA-based hydrogel scaffolds to function as cell-laden 3D environments which can be used to promote and probe vasculogenesis and angiogenesis.[25,29]

These highly modifiable materials have been used extensively to evaluate changes in formation and function of vasculature in response to pro-angiogenic growth factors, ECM proteins (i.e., fibronectin, laminin, and collagen), and their peptide mimics.[1,15,29,30] Conversely, relatively little work has assessed how the hydrogel stiffness affects angiogenesis and vasculogenesis in 3D or how these mechanical effects influence host tissue and vascularization responses. In these few studies, reducing hydrogel mechanical properties has been shown to alter vascular network characteristics such as vessel length, vessel diameter, and extent of branching.[25,34] Studies that have addressed the effects of mechanical properties on *in vivo* cell and tissue responses have indicated that PEG hydrogel stiffness influences both the inflammatory response[5] and the extent of cellular invasion into the hydrogel.[14] However, these studies controlled the hydrogel's mechanical properties by changing the polymer density or the polymer chain length, which are both directly coupled to other physical properties of the hydrogel, including the mesh size, diffusivity, and degradative properties.[19] In particular, the coupling of mechanical properties to rates of degradation make it difficult to create soft degradable materials that can persist for extended periods of time, often leading to the use of non-degradable scaffolds or high density, high stiffness materials that fail to recapitulate endogenous tissue mechanics. The reduced lifetimes of these materials makes them inadequate for many tissue engineering and regenerative medicine applications, where the rate of degradation should correspond to the time course for replacement with host cells and newly synthesized ECM.[6,13] Yet, the softer mechanical regimes have often been associated with more desirable outcomes. Therefore, to investigate the role of hydrogel stiffness on host tissue responses and vascularization in more physiologically relevant mechanical regimes, we must be able to control the hydrogel's mechanical properties independent of the polymer density or polymer chain length to achieve these soft mechanical regimes with extended hydrogel lifetimes.

We have previously described a PEGDA-based macromer that introduces allyloxycarbonyl (alloc) groups into an MMP-sensitive peptide sequence. The alloc groups are capable of competing with the terminal acrylate groups during crosslinking to alter the crosslinking structure of the hydrogel network.[32] Unlike acrylate groups, which propagate free radicals during polymerization reactions, the alloc groups tend to terminate free radical propagation.[24] This leads to fewer PEGDA chains terminating at poly(acrylate) sites, thus lowering the connectivity of the network, and reduces the overall mechanical properties of the hydrogel. Previously, we used this modification to create hydrogels with compressive moduli that could be tuned over an order of magnitude at constant polymer density and chain length while maintaining the degradative and diffusive properties of the hydrogel. Through this work, we showed that by decreasing the mechanical properties, the kinetics of endothelial cell (EC) spreading and EC assembly into vessel-like networks (i.e., vasculogenesis) were accelerated. Importantly, this demonstration indicated that these mechanically influenced effects held true independent of the polymer density or chain length and in a minimalistic environment containing only the fibronectin-derived adhesive peptide sequence Arg-Gly-Asp-Ser (RGDS).

The purpose of the current work was to test these same materials in an angiogenesis-based microvascularization system by implanting the stiff (alloc omitting, $E = 18$ kPa) and soft (alloc containing, $E = 2$ kPa) hydrogels subcutaneously in rats. These experiments would permit us to investigate how the mechanical properties of proteolytically degradable and cell adhesive PEGDA-based hydrogels affect host tissue integration and neovascularization through angiogenesis. In addition, we would examine the ability of soluble fibroblast growth factor 2 (FGF-2) and platelet derived growth factor homodimer B (PDGF BB) released from the hydrogels to improve EC recruitment from surrounding tissue, cell infiltration, and vascularization. This understanding should help to identify future biomaterial design criteria in order to improve neovascularization and tissue perfusion for tissue engineering and regenerative medicine applications.

MATERIALS AND METHODS

PEG Macromer and Hydrogel Synthesis

The peptides GGGGGPQGIWGQGGGGK (PQ) and GGGGGPQGIWGQGG-Lys(alloc)-GK [PQ(alloc)] were synthesized using standard fluorenylmethyloxycarbonyl (Fmoc) solid-phase chemistry and 1-[Bis(dimethylamino)methylene]-1*H*-1,2,3-triazolo[4,5-

b]pyridinium 3-oxid hexafluorophosphate (HATU) activation on an Apex 396 parallel synthesizer (Aapptec, Louisville, KY). Peptide products were verified *via* mass spectroscopy using a DE-Pro MALDI-MS (Applied Biosystems). The resulting peptides were PEGylated by reacting with 2.1 molar equivalents of acrylate-PEG-succinimidyl valerate (acryl-PEG-SVA; Laysan Bio, Arab, AL) in dimethyl sulfoxide with 2:1 molar excess N,N-diisopropylethylamine to acryl-PEG-SVA under inert atmosphere. PEGylated peptides were then dialyzed and lyophilized. Purity was assessed using gel permeation chromatography (GPC) equipped with an evaporative light scattering detector (Polymer Laboratories; Amherst, MA). RGDS peptides (American Peptide, Sunnyvale, CA) were conjugated with acryl-PEG-SVA (2:1 RGDS:acryl-PEG-SVA) in HEPES-buffered saline (pH 8.5) overnight at 4 °C. PEGylated RGDS was dialyzed and lyophilized. Purity was assessed *via* GPC. All PEGylated peptides were protected from light and stored at −80 °C under inert atmosphere until use.

To form hydrogels, PEG-PQ or PEG-PQ(alloc) macromers were dissolved at identical polymer densities (w/v) in HEPES-buffered saline (pH 8.3) with 1.5% (v/v) triethanolamine (HBS-TEOA), 10 μM eosin Y and 0.35% (v/v) n-vinylpyrrolidone (NVP; Sigma). To account for differences in peptide molecular weight, the PEG-peptide macromers concentrations were normalized by total molecular weight, yielding 50 mg mL^{-1} for PEG-PQ and 52 mg mL^{-1} PEG-PQ(alloc) and corresponding to 5% (w/v). The pre-polymer solution was then dropped between PDMS spacers on to clean glass slides treated with Sigmacote (Sigma, St. Louis, MO) per the manufacturer's protocol. The droplet was capped with methacrylate-functionalized cover glass (no. 1.5). Modification of the glass with methacrylate groups was performed by submerging clean cover glass in ethanol with 2% (v/v) 3-(trimethoxysilyl)propyl methacrylate for 48 h. Hydrogels were then polymerized under a white light lamp (Dolan-Jenner, Boxborough, MA; 200 mW cm^{-2}), forming covalent linkages in the methacrylate modified coverglass.

Mechanical Testing

Hydrogels (1 mm thick) were prepared from PEG-PQ or PEG-PQ(alloc) with a final polymer density of 5% (w/v) and allowed to swell overnight in PBS at 37 °C. Hydrogels were briefly rinsed with PBS to remove any unpolymerized material before mechanical testing. Compression testing was performed on a RSA III microstrain analyzer (TA Instruments, New Castle, DE) using a 15 mm plate. Samples were compressed at a constant rate of 0.003 mm s^{-1}. Since, PEG-based hydrogels are isotropic, testing was only performed in one direction.[37]

Preparation of PEG Hydrogels for In Vivo Implantation

Each hydrogel was formed from 75 μL of pre-polymer solution containing 5% (w/v) of the appropriate PEG macromer [either PEG-PQ or PEG-PQ(alloc)] and 3.5 mM PEG-RGDS in HBS-TEOA with eosin Y and NVP. The pre-polymer solution was sterilized by being passed through a 0.2 μm syringe filter (Pall Acrodisc with Supor Membrane, Pall Corporation, Port Washington, NY) then dropped between 1 mm thick spacers and polymerized for 2 min between two Sigmacote-treated glass slides. Hydrogels were placed in sterile PBS that contained or omitted 1 μg mL^{-1} FGF-2 and 5 μg mL^{-1} PDGF-BB (ProSpec-Tany TechnoGene Ltd., Rehovot, Israel), yielding an estimated equilibrium loading of ~375 ng PDGF-BB and ~75 ng FGF-2 per hydrogel. Hydrogels were incubated overnight at 37 °C to swell and take up growth factors.

Surgical Procedures for Hydrogel Implantation

All animal procedures were performed in accordance with the NIH Guide for Care and Use of Laboratory Animals as well as the Duke University Institutional Animal Care & Use Committee (IACUC). For subcutaneous implantations, 8 week old male Lewis rats (Charles River Laboratories, Wilmington, MA) were anesthetized with 2% isofluorane in O_2 and five full thickness cutaneous incisions were made (≤1 cm) in an alternating pattern along the dorsal midline of the rats. Subcutaneous pockets were then formed using blunt dissection transverse to the incisions. The hydrogels were inserted into the subcutaneous pockets following randomization of samples. Incisions were closed with interrupted nylon sutures (4-0, Santa Cruz Biotechnology, Santa Cruz, CA). After 3, 7, 14, or 28 days post-implantation, animals were euthanized and the hydrogels (with adjacent tissue) were excised for histological analysis.

Tissue Preparation

Excised tissues with hydrogels were fixed in 10% normal buffered formalin (NBF, Fisher Scientific, Waltham, MA) for 24 h at 4 °C then manually dissected into 3–5 mm thick sections, placed in NBF, and fixed for an additional 24 h at 4 °C. Samples were then transferred into Optimal Cutting Temperature (OCT) Compound (Tissue-Tek, Sakura Finetek, Torrance, CA) and left at 4 °C for 72 h. Afterwards tissues were immersed in OCT Compound in plastic molds, then

placed in an acetone/dry ice bath for 30 min. Embedded tissues were stored at −80 °C until sectioning. For sectioning, embedded molds were equilibrated at their cutting temperature (−22 °C) for 30 min then sectioned (10 μm thickness) and mounted on Superfrost Plus glass slides (Electron Microscopy Sciences, Hatfield, PA). Mounted sections were stored at −80 °C. Before staining, sections were brought to room temperature and dried overnight.

Hematoxylin & Eosin Staining

For hematoxylin & eosin (H&E) staining, sections were briefly hydrated in DI water, placed in Mayer's Hematoxylin for 2 min, and thoroughly rinsed with tap water. After rinsing, slides were stained with eosin solution for 45 s then dehydrated consecutively through a series of 75–100% ethanol solutions before a 5 min 100% ethanol incubation. Slides were then placed in Citrisolv (Fisher Scientific) for 5 min and rinsed with ethanol before being dried at room temperature. Sections were mounted with Cytoseal 60 (Richard-Allan Scientific, San Diego, CA), covered with cover glass, and allowed to dry.

Immunofluorescent Staining

For immunofluorescence, samples were rinsed with DI water then blocked for 30 min in 5% normal donkey serum followed by incubation with mouse anti-rat CD31 (BD Biosciences, San Jose, CA) or mouse anti-rat CD68 (AbD Serotec, Kidlington, UK) at a 1:200 dilution in PBS containing 0.5% normal donkey serum for 1 h. Following incubation, samples were washed three times for 5 min with PBS then incubated with Alexafluor488 conjugated donkey anti-mouse at 1:200 dilution in 0.5% normal donkey serum for 30 min. Sections were washed for 5 min in PBS, 5 min in 4′,6-diamidino-2-phenylindole solution (DAPI; Sigma, 2 μM in PBS), and 5 min in PBS then post-fixed for 15 min in 4% paraformaldehyde on ice. For all CD68 staining, TBS was substituted for PBS except for during the DAPI staining step. 1–2 drops of Fluoromount (Sigma) were applied to each section and then the sample was covered with cover glass and sealed. Samples were imaged within 48 h.

Microscopy and Image Analyses

Imaging was performed using an Axio Observer Z1 equipped with an Axiocam ICc1 (for brightfield) and an Axiocam MRm camera (for fluorescence). All images were acquired with a 10 × (0.25 NA) Fluar objective. Images were stitched together for analyses and display using Zeiss MosaiX. Image analyses were performed using ImageJ.[31] For area-based normalization, gaps or holes in the gel or tissue areas were omitted from the total area calculations.

Statistical Analyses

Statistical analyses were performed using the software package JMP Pro 11 (SAS Institute, Cary, NC). Datasets were analyzed using one-way analysis of variance (ANOVA), followed by Tukey's Honest Significant Difference test for multiple comparisons. In all cases, p-values less than 0.05 were considered significant and all values are reported as mean ± standard deviation.

RESULTS

Mechanical Characterization of Hydrogels

The PEG-PQ and PEG-PQ(alloc) hydrogels were tested under compression to verify the decrease in mechanical properties of the hydrogels due to the incorporation of the alloc group. The PEG-PQ(alloc) hydrogels exhibited a significant reduction of the compressive modulus as compared to the PEG-PQ hydrogels with 2.16 ± 0.78 kPa for PEG-PQ(alloc) and 18.47 ± 1.52 kPa for PEG-PQ, similar to the previously reported values.[32] For these studies, the mechanical regimes utilized either typify the compressive mechanics of similar photopolymerized PEGDA hydrogel systems (i.e., PEG-PQ)[16] or approximate the mechanics of endothelial tissues, in the case of the PEG-PQ(alloc) hydrogels.[8] While loading the growth factors FGF and PDGF-BB into the hydrogel may slightly alter the mechanical properties of the hydrogel, previous work shown that the loading capabilities of the hydrogels are similar and the release profile of these growth factors should be quite fast. Using the data from our earlier study, we would anticipate that over 95% of the growth factors should be released within the first 60 min to initiate a response from the surrounding tissue.[32]

Inflammation Response to Implanted Hydrogels

To evaluate the local inflammatory response to the implanted hydrogels, the extent of macrophage recruitment was quantified. For these analyses, macrophages were identified *via* positive staining for CD68. The acquired fluorescence images showed that > 95% of the CD68 positive cells were within 150 μm of the implanted hydrogels at all time points measured, so this banded region surrounding the hydrogel was chosen to evaluate the macrophage

density and recruitment response (Figs. 1a and S1). After 3 days *in vivo*, the different hydrogel formulations displayed no significant difference in macrophage density [PEG-PQ: 442.1 ± 206.9; PEG-PQ(alloc): 441.6 ± 181.7; PEG-PQ w/growth factors: 479.1 ± 290.0; and PEG-PQ(alloc) w/growth factors: 385.9 ± 182.4 macrophages mm^{-2}]. After 7 days *in vivo*, there was no observed change in macrophage density [PEG-PQ: 307.5 ± 186.8; PEG-PQ(alloc): 575.0 ± 200.6; PEG-PQ w/growth factors: 478.2 ± 197.0; and PEG-PQ(alloc) w/growth factors: 368.4 ± 181.1 macrophages mm^{-2}] (Fig. 1b). These results indicate that the material compliance in the regimes we tested and the hydrogel formulation/crosslinking does not alter the local macrophage recruitment response. For comparison, these macrophage densities equate to between 22.5 (300 macrophages mm^{-2}) and 45 (600 macrophages mm^{-2}) macrophages per field of view as seen in Figs. 1 and S1. While an optimal macrophage density is difficult to establish, similar densities have been previously reported that correlated with effective tissue infiltration and vessel formation in implanted hydrogels.[36]

Host Tissue Response to Hydrogel Compliance

The extent of tissue integration into the implanted hydrogels was evaluated using H&E stained sections. After 14 days implantation *in vivo*, all hydrogels showed some level of tissue integration. The stiffer PEG-PQ hydrogels without growth factors displayed the least amount of interaction with the surrounding tissue, exhibiting distinct boundaries between the hydrogel and tissue (Fig. 2a). The softer PEG-PQ(alloc) hydrogels without growth factors showed many tissue projections into the hydrogels with extensive branching. A few thicker tissue segments could also be observed (Fig. 2b). When growth factors were added, the PEG-PQ hydrogels showed more extensive interactions with the surrounding tissue. Here, several tissue projections could be seen ranging from 25 to 50 μm accompanied by thinner projections (Fig. 2c). Similarly, the PEG-PQ(alloc) hydrogels with growth factors showed a large number of the thicker tissue projections into the hydrogels with thinner branching structures that could be found throughout the hydrogel (Fig. 2d). After 4 weeks, all hydrogel formulations showed increased interaction with the surrounding tissue. The PEG-PQ hydrogels without growth factors still had regions with distinct boundaries between tissue and hydrogel, but now had noticeable tissue segments that had infiltrated the hydrogel (Fig. 3a). The PEG-PQ(alloc) hydrogels without growth factors also showed an increase in tissue infiltrations now with noticeably more thicker tissue segments (Fig. 3b). When growth factors were incorporated, the PEG-PQ hydrogels also showed some increased tissue integration compared to the 14 day time point (Fig. 3c). However, the softer PEG-PQ(alloc) hydrogel with growth factors exhibited extensive host tissue integration throughout the hydrogel area (Fig. 3d).

These observations could be quantified by determining the area fraction of the tissue segments found within the hydrogel boundary to the total hydrogel area. For these analyses, the hydrogel boundary was identified by the deep blue staining due to uptake of the hematoxylin stain, which could easily be identified in all H&E images (Figs. 2 and 3) and quantified by tissue area fraction (TAF) Eq. (1).

$$\mathrm{TAF} = \frac{A_T}{A_H + A_T} \tag{1}$$

where A_T is the area of the tissue within the hydrogel and A_H is the area of the hydrogel. Here, the TAFs largely agreed with the gross observations. After 14 days, the PEG-PQ hydrogels without growth factors showed significantly lower TAFs (0.0092 ± 0.0092) than the PEG-PQ(alloc) hydrogels (without growth factors: 0.0855 ± 0.0070; and with growth factors: 0.1162 ± 0.0225) and a similar response to the PEG-PQ hydrogels w/growth factors (0.0544 ± 0.0427). After 28 days, the PEG-PQ(alloc) hydrogels with and without growth factors showed similar TAFs (0.1644 ± 0.0233 and 0.1360 ± 0.0405, respectively) that were significantly higher than their corresponding PEG-PQ hydrogel (0.0618 ± 0.0339 for PEG-PQ and 0.0885 ± 0.0192 for PEG-PQ with growth factors; Fig. 4a). When the tissue segments that infiltrated the hydrogels were measured, the PEG-PQ hydrogels without growth factors had significantly shorter lengths than the other hydrogels (Fig. 4b).

Hydrogel Promoted Microvascularization

H&E staining was used to identify microvessels both within the hydrogel area as well as within 150 μm of the tissue/hydrogel interface. Microvessel structures within the hydrogel must have resulted from cell-based degradation of the hydrogel followed by cell migration into the hydrogel area and subsequent formation of lumenized structures. In contrast, microvessels in the area surrounding hydrogel area are a result of either extensive degradation of the hydrogel and replacement by new vascularized tissue or the creation of a pro-angiogenic environment surrounding the hydrogel. In both cases microvessels could be identified as lumenized structures that contained erythrocytes. The number of microvessels in each of the hydrogel formulations in these regions was counted and normalized

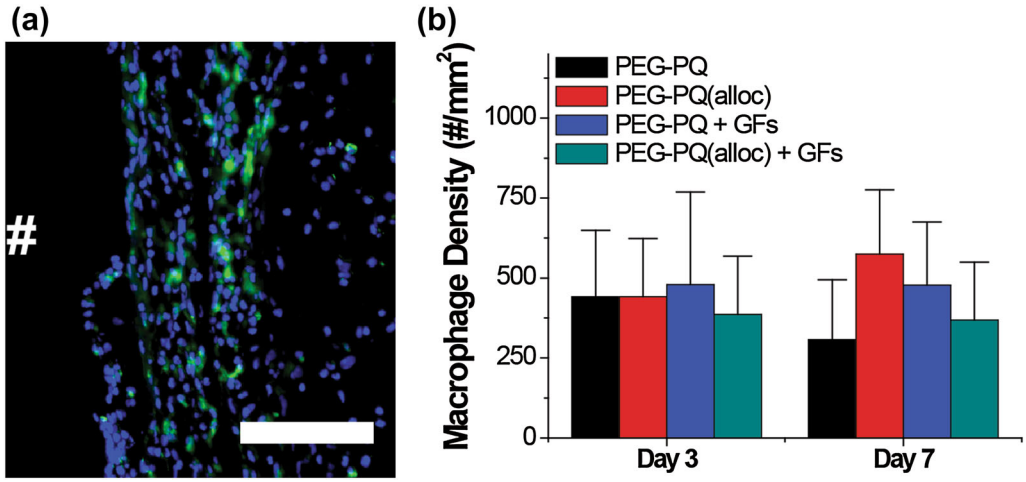

FIGURE 1. Macrophage response to implanted PEG-based hydrogels. (a) Fluorescence image of CD68 (green) and DAPI (blue) stained tissue section, showing localization of CD68+ macrophages remaining within 150 μm of the hydrogel–tissue interface. # indicates the location of the hydrogel in reference to the tissue; scale bar represents 100 μm. (b) Quantification of the macrophage density within the 150 μm deep band surrounding the hydrogel–tissue interface across all hydrogel formulations at days 3 and 7. No Significant differences were observed ($N = 4$).

to the area. The microvessel density generally correlated with the extent of tissue integration into the hydrogels (Figs. 2 and 3, yellow arrows). In these evaluations, PEG-PQ(alloc) hydrogels with growth factors exhibited significantly higher microvessel densities than the hydrogels that lacked growth factor and a similar response to the PEG-PQ hydrogels with growth factors. After 28 days, the PEG-PQ(alloc) hydrogels exhibited significantly higher microvessel densities than their PEG-PQ counterparts. Interestingly, the PEG-PQ(alloc) hydrogels that omitted growth factors saw similar microvessel densities to the stiffer PEG-PQ hydrogels that contained growth factors. In all cases, only the PEG-PQ(alloc) hydrogels experienced a sustained microvascularization response over the course of the experiments (Fig. 5a). When the area surrounding the hydrogels was examined, no difference was observed amongst any of the hydrogel formulations after 14 days. After 28 days, the PEG-PQ(alloc) hydrogels that contained growth factors showed a significant increase in microvessel density within the hydrogel over the other hydrogels (Fig. 5b). While H&E staining could inform us of the interactions of the material with the surrounding tissue, it could not help to identify information about the cells themselves. Therefore, we stained tissue sections for the EC marker CD31. Using immunohistochemistry we could see that the vast majority of cells that infiltrated into the hydrogel were CD31 positive (Fig. 6). Here, the apparent density of CD31 positive cells is similar in both gel types in the infiltrating segments.

DISCUSSION

We previously demonstrated a method to alter the mechanical properties of cell adhesive and proteolytically-degradable PEGDA-based hydrogels through changes to the cross-linking structure as opposed to polymer density or polymer chain length. Changes to the crosslinking structure were introduced *via* the incorporation of a Lys(alloc) amino acid on the carboxy terminus of the MMPs 2 and 9 cleavable PQ sequence. The alloc group can then act as a competitive crosslinking site during photopolymerization to alter the connectivity of PEGDA-based hydrogels. The different crosslinked structures that arise from differences in free radical propagation between acrylate and alloc groups reduces the stiffness of the hydrogel independent of the diffusive or degradative properties. The compressive moduli of the resulting hydrogels could be tuned by changing the concentration of alloc-containing PEG macromers in the pre-polymer solution. Using this modification, we demonstrated that ECs respond to the mechanical properties of the hydrogel environment both through enhanced spreading and network formation kinetics. From these studies, we have shown that this hydrogel system can act as a functional platform to assay mechanical influences in various biological settings. Here, we sought to use this cell adhesive and proteolytically degradable hydrogel platform to better understand the role of hydrogel mechanics on neovascularization *in vivo*. We hypothesized that this hydrogel system should allow us to evaluate the role of hydrogel

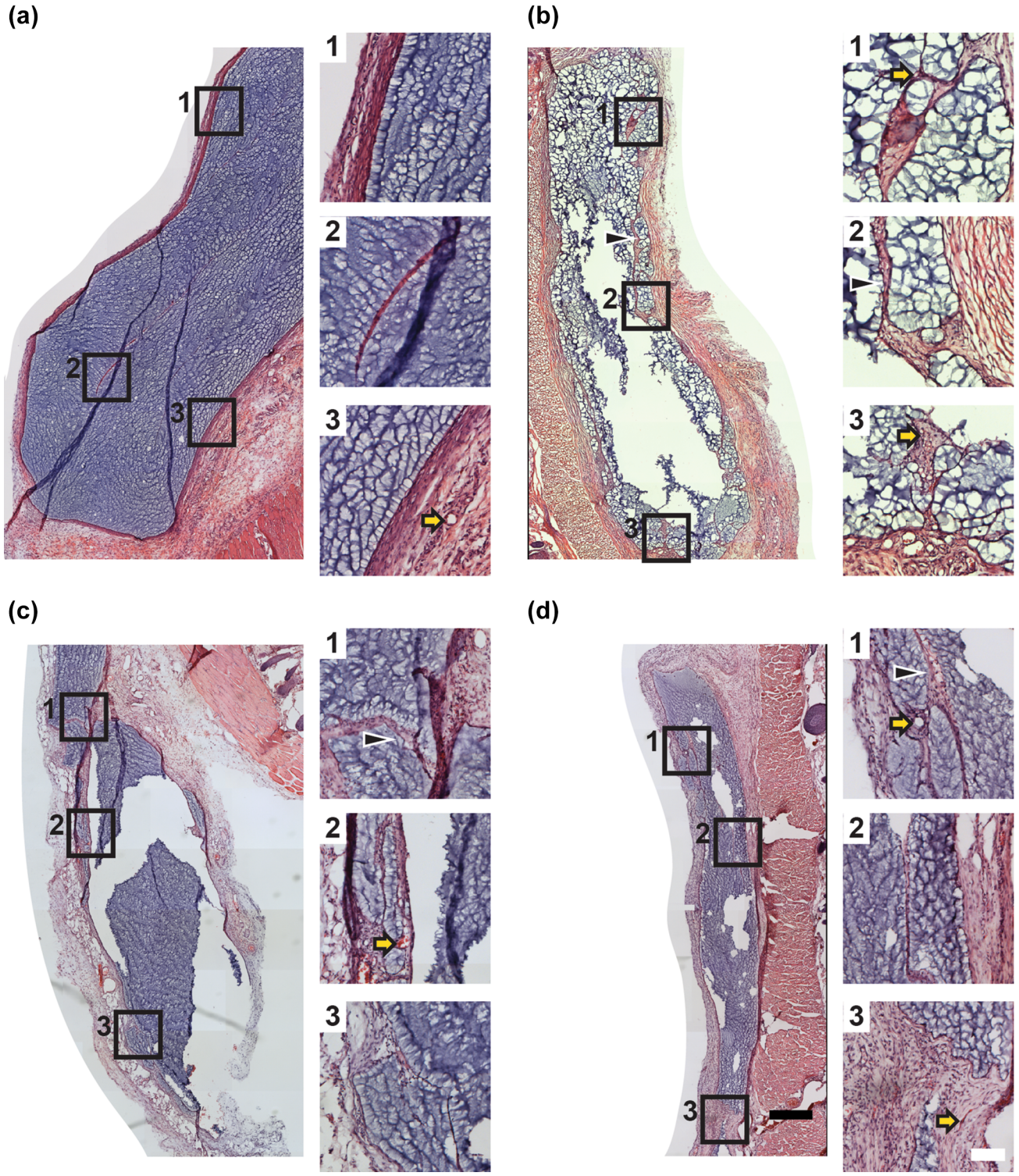

FIGURE 2. H&E stained tissue sections of (a) PEG-PQ; (b) PEG-PQ(alloc); (c) PEG-PQ w/growth factors; and (d) PEG-PQ(Alloc) w/growth factors after 14 days *in vivo*. Yellow arrows indicate the location of microvessels, black arrowheads indicate thick tissue segments within the hydrogels. Black scale bar for the large format images represents 500 μm and the white scale bar for the zoomed in images represents 100 μm. Zoomed in regions better illustrating the microvessels can be found in Fig. S2.

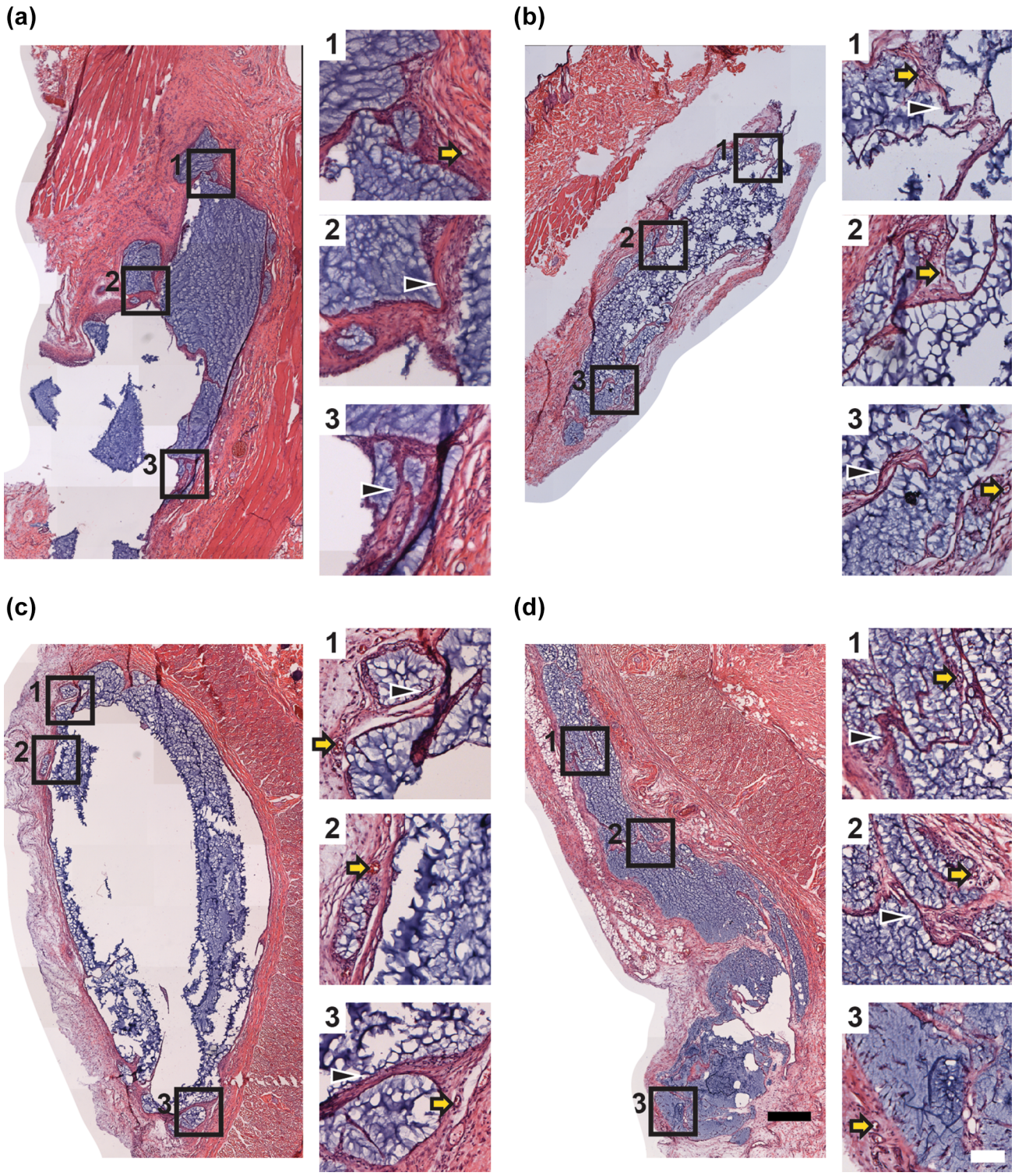

FIGURE 3. H&E stained tissue sections of (a) PEG-PQ; (b) PEG-PQ(alloc); (c) PEG-PQ w/growth factors; and (d) PEG-PQ(Alloc) w/growth factors after 28 days *in vivo*. Yellow arrows indicate the location of microvessels, black arrowheads indicate thick tissue segments within the hydrogels. Black scale bar for the large format images represents 500 μm and the white scale bar for the zoomed in images represents 100 μm. Zoomed in regions better illustrating the microvessels can be found in Fig. S2.

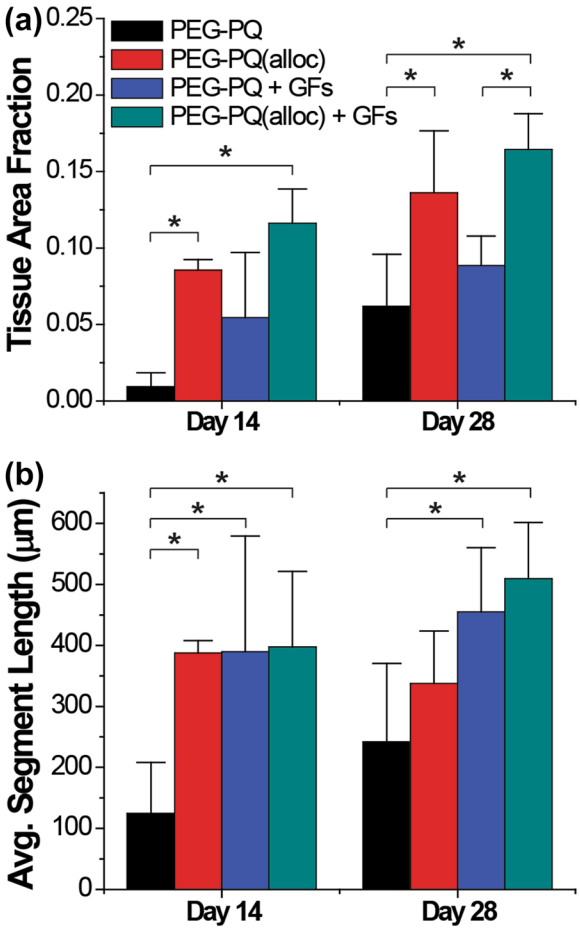

FIGURE 4. Quantification of the tissue segments infiltrating the hydrogels at days 14 and 28. (a) The ratio of tissue area to total hydrogel area was calculated for all hydrogel formulations. Alloc containing hydrogels showed the greatest tissue area fractions at both 14 and 28 days. (b) When the segments were individually measured, PEG-PQ hydrogels had the shortest segments after 14 days. After 28 days, only growth factor containing hydrogels exhibited longer segment lengths than the blank PEG-PQ hydrogels. *Significant differences ($p < 0.05$; $N = 4–5$).

mechanics on host tissue integration and microvascularization while maintaining other physical characteristics of the hydrogels across all conditions.

While tissue mechanics are known to contribute to development and the determination of local cell phenotypes,[12,22] very little work has been done to investigate the role of biomaterial mechanical properties on their ability to function and interact with cells *in vivo*. Studies that have attempted to understand how material stiffness influences host tissue interactions using PEG-based hydrogels have generally shown that softer hydrogels minimize inflammation and promote tissue induction.[5,14] However, similar to many *in vitro* investigations, lowering the hydrogel's mechanical properties was achieved by reducing the polymer density, which either sped up the rate of degradation or necessitated the use of non-degradable materials. For example, Ehrbar *et al*. observed the greatest amount of cell invasion into their softest hydrogels produced *via* transglutaminase crosslinking of multi-armed PEG.[14] However, the gel mechanics were reduced by lowering the polymer density, making it difficult to decouple the effects of polymer density from hydrogel mechanics or evaluate how the material is perceived by the surrounding tissue. Similarly, once the hydrogel density was sufficiently low, proteolysis of the polymer backbone was no longer necessary to permit cellular migration, suggesting that the changes to matrix density significantly altered other properties of the hydrogel, such as the resulting hydrogel mesh size. In another study by Blakney *et al*., reducing the stiffness of PEGDA hydrogels led to a reduction in the macrophage response at the hydrogel–tissue interface.[5] However, the hydrogel's mechanical properties were altered by decreasing the polymer density. Additionally, the PEGDA macromers that were used were not proteolytically degradable nor should they be degradable by hydrolysis over the time course studied.[4,7] Therefore, the use of crosslinking structure to control hydrogel mechanics and evaluate host tissue interactions should garner a better perspective on these substrate stiffness dependent behaviors.

In the current work, a subcutaneous implantation model in rats was chosen as this has been an effective model to evaluate host interactions with implanted biomaterials, particularly in the cases of angiogenesis and inflammation.[27,33] In contrast to our previous work, the hydrogels were polymerized without the incorporation of cells, requiring the recruitment of host ECs to form new microvasculature *via* angiogenesis. However, the endogenous vasculature and ECs are generally quiescent, often requiring a stimulus to form new vessels.[9] Therefore, we incorporated local growth factor release to activate the nearby ECs to form new microvessels and infiltrate the hydrogel environment. We tested this by loading some of the hydrogels with a combination of FGF-2 and PDGF-BB, which have previously been shown to act as effective chemo-attractants, aiding in the formation of microvasculature *in vitro* and *in vivo*.[10,30] Both the PEG-PQ and PEG-PQ(alloc) hydrogels that contained growth factors exhibited increased microvessel formation at the 2 week time point compared to their counterparts that lacked growth factors. At 4 weeks, though, only the softer PEG-PQ(alloc) hydrogels showed enhancements in microvessel density. Our previous work would suggest that the growth factors are completely released within a few hours in an aqueous environment.[30,32] We anticipate that the *in vivo* release would similarly be quite fast, but sequestration of the growth factors by the ECM may

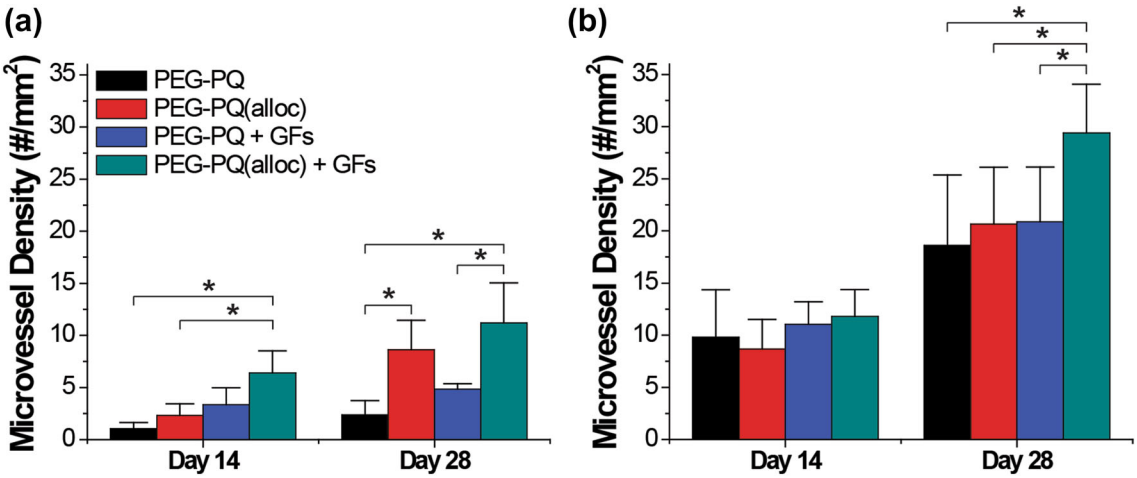

FIGURE 5. Microvessel density was calculated for areas (a) inside and (b) surrounding the hydrogels. (a) At early time points within the hydrogel area, PEG-PQ(alloc) and PEG-PQ hydrogels that contained growth factors showed higher densities than the PEG-PQ hydrogel alone. The PEG-PQ(alloc) response was consistent with the PEG-PQ hydrogels that contained growth factors. After 28 days, both PEG-PQ(alloc) hydrogels showed increased microvessel density compared to the PEG-PQ hydrogels. (b) The area around the hydrogels showed no difference between formulations after 14 days, but the PEG-PQ(alloc) hydrogels with growth factors showed increased microvessel density compared to the other groups. * indicate significant differences ($p < 0.05$; $N = 4–5$).

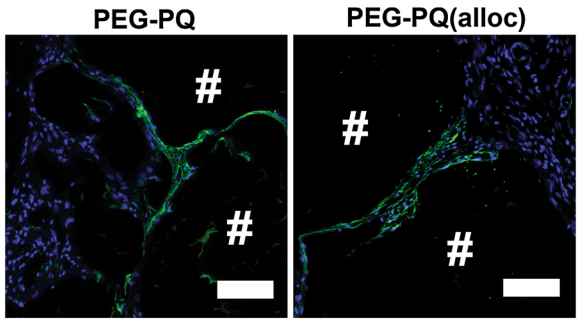

FIGURE 6. Fluorescence staining of hydrogel sections for ECs for the EC marker CD31. CD31 (green) and DAPI (blue) staining showing positive staining of tissue segments integrating into PEG-PQ (left) and PEG-PQ(alloc) (right) hydrogels after 4 weeks of implantation. Both hydrogel types exhibit similar densities of CD31 positive cells in the integrating segments, indicating the extent of tissue integration should correlate to neovascularization. # indicates the location of the hydrogel in reference to the tissue, scale bar represents 100 μm.

help to sustain a local increase in the growth factor concentrations. This is likely depleted within the 2 weeks though, leading to only a short term improvement in microvascularization. This is consistent with a previous study that showed after a depot of growth factor is depleted, the functional benefits quickly end.[28] This result may then indicate that the compliance of the hydrogels helps to not only promote microvessel formation, but also helps to maintain this positive response over a longer time course.

Substrate stiffness has been shown to regulate MMP production and activation in multiple cell types,[18] including fibroblasts and ECs, which are present within and around the implanted hydrogels. However, these changes in MMP levels are generally a result of dynamic mechanical processes such as stress relaxation events[20] or the application of cyclical strain or shear stress,[3,38] as opposed to a static matrix rigidity. In our work, the stiffer hydrogels exhibit a much more delineated barrier between the hydrogel and the local tissue as compared to the more compliant alloc-containing gels. This would suggest that the decreased hydrogel stiffness should either influence MMP secretion by local cells, the activation of pro-MMPs, or alter the rate of degradation by MMPs resulting in a greater extent of cellular invasion into the hydrogel. It has been postulated that cellular remodeling can be dictated by matrix mechanics,[11] indicating that the mechanical properties of the material could influence the rate and extent of proteolytic degradation from the cells and tissue. While the mechanism by which this should occur is unclear, our data would suggest that the mechanical properties of cell-scaffold interactions may influence elements of MMP-based proteolysis and remodeling. In this case, we would anticipate the hydrogel mechanics are the determinant factor as the biochemical cues (i.e., PEG-RGDS concentration) within the hydrogel are identical and the local tissue makeup exhibits similar microvessel and macrophage densities in the regions surrounding the hydrogels.

A potential alternative to this explanation is that the compliant PEG-PQ(alloc) hydrogels exhibit differential inflammatory responses than the stiffer PEG-PQ hydrogels. Inflammation has been known to influence angiogenesis and vascularization, having the ability to enhance or inhibit these responses.[35,36] Inflammatory responses to photopolymerizable PEG-based hydro-

gels are largely attributed to the hydrophobic acrylate crosslinking sites formed during the polymerization process. Given the change in crosslinking structure imparted by the alloc groups, the PEG-PQ(alloc) hydrogels may exhibit a very different inflammatory response. Using CD68 staining for macrophages, we did not observe any significant differences in macrophage-induced inflammation across the hydrogel formulations. Macrophages can further be classified by their phenotype (i.e., M1, M2, and their subgroups) which have been suggested to correlate with pro-angiogenic outcomes. Yet these pro-angiogenic outcomes have been observed in all macrophage phenotypes, so they are not currently an effective indicator of neovascularization responses.[35] While previous work has suggested that macrophage recruitment is influenced by the mechanical properties of PEGDA hydrogels,[5] this work utilized short PEGDA macromers which resulted in significantly stiffer hydrogels, ranging from 130 to 840 kPa, than those used here, which range from 2 to 18 kPa. This may suggest a reduction in macrophage response until a threshold stiffness is achieved or that the difference in the mechanical properties between the PEG-PQ and PEG-PQ(alloc) hydrogels was not sufficient to elucidate a change in macrophage recruitment. Similarly, the PEGDA hydrogels in the previous study were non-degradable, so the proteolytic degradability of our hydrogels may also contribute to the lack of a quantifiable macrophage response. While the presence of the cell adhesive PEG-RGDS ligand may also play a role in mediating local inflammation, previous work has suggested that the incorporation of RGDS into PEGDA hydrogels leads to decreases in the macrophage recruitment response.[21] Due to these data and the existing literature, we do not believe that inflammation is the determining factor in the observed neovascularization responses.

By incorporating or omitting the competitive alloc crosslinking sites we could modulate the mechanical properties exhibited by these hydrogel independently of their polymer density or chain length. This change in the hydrogel crosslinking structure effectively decoupled the hydrogel's mechanical properties from other physical parameters, such as degradability and diffusivity, creating mechanical environments that better match those of endothelial tissues.[8] Our work indicates that the mechanical properties of these proteolytically degradable PEGDA hydrogels play a critical role in how the hydrogel interacts with the local tissue environment. Here, this decreased stiffness leads to increased microvascularization and tissue integration for at least four weeks *in vivo*. This demonstration reinforces the primary idea that approximating the local tissue environment should improve biomaterial outcomes for regenerative therapies.

ELECTRONIC SUPPLEMENTARY MATERIAL

The online version of this article (doi: 10.1007/s10439-017-1822-8) contains supplementary material, which is available to authorized users.

ACKNOWLEDGMENTS

The authors thank Drs. Suzana Vellejo-Heligon, Nga Le Brown, and Mohamed Ibrahim for helpful discussions. This work was supported by grants from the National Institutes of Health R01EB16629 (to JLW) and F32HL120650 (to RMS) and a Post-Doctoral Fellowship from Regeneration Next Initiative at Duke University (to RMS).

REFERENCES

[1]Ali, S., J. E. Saik, D. J. Gould, M. E. Dickinson, and J. L. West. Immobilization of cell-adhesive laminin peptides in degradable PEGDA hydrogels influences endothelial cell tubulogenesis. *Bioresour. Open Access*. 2:241–249, 2013.

[2]Bajaj, P., R. M. Schweller, A. Khademhosseini, J. L. West, and R. Bashir. 3D biofabrication strategies for tissue engineering and regenerative medicine. *Annu. Rev. Biomed. Eng*. 16:247–276, 2014.

[3]Bassiouny, H. S., R. H. Song, X. F. Hong, A. Singh, H. Kocharyan, and S. Glagov. Flow regulation of 72-kD collagenase IV (MMP-2) after experimental arterial injury. *Circulation* 98:157–163, 1998.

[4]Benoit, D. S., A. R. Durney, and K. S. Anseth. Manipulations in hydrogel degradation behavior enhance osteoblast function and mineralized tissue formation. *Tissue Eng*. 12:1663–1673, 2006.

[5]Blakney, A. K., M. D. Swartzlander, and S. J. Bryant. The effects of substrate stiffness on the in vitro activation of macrophages and in vivo host response to poly(ethylene glycol)-based hydrogels. *J. Biomed. Mater. Res. A*. 100: 1375–1386, 2012.

[6]Brandl, F., F. Sommer, and A. Goepferich. Rational design of hydrogels for tissue engineering: impact of physical factors on cell behavior. *Biomaterials* 28:134–146, 2007.

[7]Browning, M. B., and E. Cosgriff-Hernandez. Development of a biostable replacement for PEGDA hydrogels. *Biomacromolecules* 13:779–786, 2012.

[8]Butcher, D. T., T. Alliston, and V. M. Weaver. A tense situation: forcing tumour progression. *Nat. Rev. Cancer* 9:108–122, 2009.

[9]Campagnolo, L., A. Leahy, S. Chitnis, S. Koschnick, M. J. Fitch, J. T. Fallon, D. Loskutoff, M. B. Taubman, and H. Stuhlmann. EGFL7 is a chemoattractant for endothelial cells and is up-regulated in angiogenesis and arterial injury. *Am. J. Pathol*. 167:275–284, 2005.

[10]Cao, R., E. Brakenhielm, R. Pawliuk, D. Wariaro, M. J. Post, E. Wahlberg, P. Leboulch, and Y. Cao. Angiogenic synergism, vascular stability and improvement of hind-limb ischemia by a combination of PDGF-BB and FGF-2. *Nat. Med.* 9:604–613, 2003.
[11]Dikovsky, D., H. Bianco-Peled, and D. Seliktar. Defining the role of matrix compliance and proteolysis in three-dimensional cell spreading and remodeling. *Biophys. J.* 94:2914–2925, 2008.
[12]Discher, D. E., P. Janmey, and Y. L. Wang. Tissue cells feel and respond to the stiffness of their substrate. *Science* 310:1139–1143, 2005.
[13]Drury, J. L., and D. J. Mooney. Hydrogels for tissue engineering: scaffold design variables and applications. *Biomaterials* 24:4337–4351, 2003.
[14]Ehrbar, M., A. Sala, P. Lienemann, A. Ranga, K. Mosiewicz, A. Bittermann, S. C. Rizzi, F. E. Weber, and M. P. Lutolf. Elucidating the role of matrix stiffness in 3D cell migration and remodeling. *Biophys. J* . 100:284–293, 2011.
[15]Garcia, J. R., A. Y. Clark, and A. J. Garcia. Integrin-specific hydrogels functionalized with VEGF for vascularization and bone regeneration of critical-size bone defects. *J. Biomed. Mater. Res. A*. 104:889–900, 2016.
[16]Gill, B. J., D. L. Gibbons, L. C. Roudsari, J. E. Saik, Z. H. Rizvi, J. D. Roybal, J. M. Kurie, and J. L. West. A synthetic matrix with independently tunable biochemistry and mechanical properties to study epithelial morphogenesis and EMT in a lung adenocarcinoma model. *Cancer Res.* 72:6013–6023, 2012.
[17]Hsu, C. W., R. M. Olabisi, E. A. Olmsted-Davis, A. R. Davis, and J. L. West. Cathepsin K-sensitive poly(ethylene glycol) hydrogels for degradation in response to bone resorption. *J. Biomed. Mater. Res. A* 98:53–62, 2011.
[18]Humphrey, J. D., E. R. Dufresne, and M. A. Schwartz. Mechanotransduction and extracellular matrix homeostasis. *Nat. Rev. Mol. Cell Biol.* 15:802–812, 2014.
[19]Kloxin, A. M., C. J. Kloxin, C. N. Bowman, and K. S. Anseth. Mechanical properties of cellularly responsive hydrogels and their experimental determination. *Adv. Mater.* 22:3484–3494, 2010.
[20]Lambert, C. A., A. C. Colige, C. Munaut, C. M. Lapiere, and B. V. Nusgens. Distinct pathways in the over-expression of matrix metalloproteinases in human fibroblasts by relaxation of mechanical tension. *Matrix Biol.* 20:397–408, 2001.
[21]Lynn, A. D., T. R. Kyriakides, and S. J. Bryant. Characterization of the in vitro macrophage response and in vivo host response to poly(ethylene glycol)-based hydrogels. *J. Biomed. Mater. Res. A* 93:941–953, 2010.
[22]Mammoto, T., and D. E. Ingber. Mechanical control of tissue and organ development. *Development* 137:1407–1420, 2010.
[23]Mann, B. K., R. H. Schmedlen, and J. L. West. Tethered-TGF-beta increases extracellular matrix production of vascular smooth muscle cells. *Biomaterials* 22:439–444, 2001.
[24]Matsumoto, A., T. Kumagai, H. Aota, H. Kawasaki, and R. Arakawa. Reassessment of free-radical polymerization mechanism of allyl acetate based on end-group determination of resulting oligomers by MALDI-TOF-MS spectrometry. *Polym. J.* 41:26–33, 2009.
[25]Moon, J. J., J. E. Saik, R. A. Poche, J. E. Leslie-Barbick, S. H. Lee, A. A. Smith, M. E. Dickinson, and J. L. West. Biomimetic hydrogels with pro-angiogenic properties. *Biomaterials* 31:3840–3847, 2010.
[26]Nguyen, K. T., and J. L. West. Photopolymerizable hydrogels for tissue engineering applications. *Biomaterials* 23:4307–4314, 2002.
[27]Nillesen, S. T., P. J. Geutjes, R. Wismans, J. Schalkwijk, W. F. Daamen, and T. H. van Kuppevelt. Increased angiogenesis and blood vessel maturation in acellular collagen-heparin scaffolds containing both FGF2 and VEGF. *Biomaterials* 28:1123–1131, 2007.
[28]Norton, L. W., H. E. Koschwanez, N. A. Wisniewski, B. Klitzman, and W. M. Reichert. Vascular endothelial growth factor and dexamethasone release from nonfouling sensor coatings affect the foreign body response. *J. Biomed. Mater. Res. A*. 81:858–869, 2007.
[29]Phelps, E. A., N. Landazuri, P. M. Thule, W. R. Taylor, and A. J. Garcia. Bioartificial matrices for therapeutic vascularization. *Proc. Natl Acad. Sci. U.S.A.* 107:3323–3328, 2010.
[30]Saik, J. E., D. J. Gould, E. M. Watkins, M. E. Dickinson, and J. L. West. Covalently immobilized platelet-derived growth factor-BB promotes angiogenesis in biomimetic poly(ethylene glycol) hydrogels. *Acta Biomater.* 7:133–143, 2011.
[31]Schneider, C. A., W. S. Rasband, and K. W. Eliceiri. NIH image to ImageJ: 25 years of image analysis. *Nat. Methods* 9:671–675, 2012.
[32]Schweller, R. M., and J. L. West. Encoding hydrogel mechanics via network cross-linking structure. *ACS Biomater. Sci. Eng.* 1:335–344, 2015.
[33]Sieminski, A. L., and K. J. Gooch. Biomaterial–microvasculature interactions. *Biomaterials* 21:2232–2241, 2000.
[34]Singh, R. K., D. Seliktar, and A. J. Putnam. Capillary morphogenesis in PEG-collagen hydrogels. *Biomaterials* 34:9331–9340, 2013.
[35]Spiller, K. L., R. R. Anfang, K. J. Spiller, J. Ng, K. R. Nakazawa, J. W. Daulton, and G. Vunjak-Novakovic. The role of macrophage phenotype in vascularization of tissue engineering scaffolds. *Biomaterials* 35:4477–4488, 2014.
[36]Tous, E., H. M. Weber, M. H. Lee, K. J. Koomalsingh, T. Shuto, N. Kondo, J. H. Gorman, 3rd, D. Lee, R. C. Gorman, and J. A. Burdick. Tunable hydrogel–microsphere composites that modulate local inflammation and collagen bulking. *Acta Biomater.* 8:3218–3227, 2012.
[37]Tseng, H., D. S. Puperi, E. J. Kim, S. Ayoub, J. V. Shah, M. L. Cuchiara, J. L. West, and K. J. Grande-Allen. Anisotropic poly(ethylene glycol)/polycaprolactone hydrogel-fiber composites for heart valve tissue engineering. *Tissue Eng. Part A* 20:2634–2645, 2014.
[38]Von Offenberg Sweeney, N., P. M. Cummins, E. J. Cotter, P. A. Fitzpatrick, Y. A. Birney, E. M. Redmond, and P. A. Cahill. Cyclic strain-mediated regulation of vascular endothelial cell migration and tube formation. *Biochem. Biophys. Res. Commun.* 329:573–582, 2005.
[39]West, J. L., and J. A. Hubbell. Polymeric biomaterials with degradation sites for proteases involved in cell migration. *Macromolecules* 32:241–244, 1999.